ELSEVIER

Available online at www.sciencedirect.com
SCIENCE DIRECT®

Solid State Ionics 165 (2003) 269–277

SOLID STATE IONICS

www.elsevier.com/locate/ssi

Switching behavior of the Prussian blue–indium hexacyanoferrate electrochromic device using the K^+-doped poly-AMPS electrolyte

Yu-Hsien Huang, Lin-Chi Chen, Kuo-Chuan Ho*

Department of Chemical Engineering, National Taiwan University, Taipei 10617, Taiwan

---

Abstract

Upon sandwiching a K^+-doped solid polymer electrolyte (SPE) in between the Prussian blue (PB) and indium hexacyanoferrate (InHCF) thin films, a precoloring-free electrochromic device (ECD), undergoing reversible blue-to-yellowish electrochromism when charged, was fabricated and studied. The K^+-doped SPE was prepared through dissolving KCl into the monomer solution of 2-acrylamido-2-methylpropane sulfonic acid (AMPS), which was then polymerized to form the KCl-doped poly-AMPS (PAMP). It was demonstrated that this ECD shows better at-rest stability than a precolored system. Also, it was found that the KCl doping level of SPE (defined by the molar ratio of KCl to AMPS, (KCl)/(AMPS)) affects the electrochemical behaviors of PB and InHCF in different ways. Thus, the KCl doping level was optimized for attaining ECD's best performances. It was found that the widest transmittance window, fastest response, and highest coloration efficiency are obtained when (KCl)/(AMPS) = 0.220, while it is the saturated doping level leads to the longest cycle life. In brief, this work aims at optimizing the design on the K^+-SPE-based PB–InHCF ECD.

PACS: 78.20 Jq

Keywords: Electrochromic device (ECD); Indium hexacyanoferrate (InHCF); Poly-2-acrylamido-2-methylpropane sulfonic acid (PAMPS); Solid polymer electrolyte (SPE); Prussian blue (PB)

---

1. Introduction

The electroactive compounds that feature redox-dependent optical properties are referred to as electrochromic (EC) materials [1]. Frequently, EC materials are prepared as thin films and coated on optically transparent electrodes, so they can be assembled into a battery-like electrochromic device (ECD) upon sandwiching an electrolyte in between [2]. The ECDs can function as electrochemically induced optical switches and promise many commercially viable applications, including displays [3], anti-glare mirrors [4], eyeglasses [5], and solar-attenuated windows [6]. On the ECD development, the cathodically coloring tungsten oxide (WO_3) has been considered as one of the best working electrodes [7–9]. In combination with anodically coloring counterelectrodes, many WO_3-based complementary ECDs, such as WO_3-Prussian blue (PB) ECDs [10–12] and WO_3-polyaniline ECDs [13,14], have been extensively investigated. Nevertheless, precoloring (or prepolarizing) the initially colorless WO_3 film to its blue reduced state (M_xWO_3, where $M^+ = H^+$ or Li^+) is usually necessary while assembling the above-mentioned WO_3-based devices. And such a precoloring step has been found to be

---

* Corresponding author. Fax: +886-2-2362-3040.
E-mail address: kcho@ntu.edu.tw (K.-C. Ho).

0167-2738/$ - see front matter © 2003 Elsevier B.V. All rights reserved.
doi:10.1016/j.ssi.2003.08.039

responsible for ECD's at-rest instability, as judged by the gradual narrowing on the transmittance window during darkened-state storage [15]. To eliminate the precoloring-induced instability, we recently fabricated a precoloring-free device based on PB and indium hexacyanoferrate (InHCF), namely PIECD [16].

The working electrode in the precoloring-free PIECD is PB (iron hexacyanoferrate, $KFe[Fe(CN)_6]$), which undergoes a reversible, blue-to-colorless color change when reduced to Everitt's salt (ES, $K_2Fe[Fe(CN)_6]$) in the presence of potassium ions [17–20]. It is widely accepted that the EC switching of PB corresponds to the following redox insertion reaction:

$$\mathrm{KFe[Fe(CN)_6](PB,\ blue)} + \mathrm{K^+} + \mathrm{e^-} \leftrightarrow \mathrm{K_2Fe[Fe(CN)_6](ES,\ colorless)} \quad (1)$$

Being an analogue of PB, InHCF ($In[Fe(CN)_6]$) is thought to undergo a redox process similar to Eq. (1) when contacting with a K^+-containing electrolyte and shows a colorless-to-yellowish switching during oxidation, as formulated in Eq. (2) [21–23]:

$$\mathrm{In[Fe(CN)_6](InY,\ yellowish)} + \mathrm{K^+} + \mathrm{e^-} \leftrightarrow \mathrm{KIn[Fe(CN)_6](InW,\ colorless)} \quad (2)$$

For the convenience of explanation, InY and InW, abbreviation for "indium yellow" and "indium white", denote the oxidized InHCF and the reduced InHCF, respectively. With such a light EC property, InHCF can serve as the pseudo-transparent counter-electrode [24]. Therefore, the PIECD assembly is precoloring-free. From Eqs. (1) and (2), the overall EC reaction for a PIECD can be written as follows:

$$\underset{\mathrm{(blue)}}{\mathrm{KFe[Fe(CN)_6]}} + \mathrm{KIn[Fe(CN)_6]} \leftrightarrow \mathrm{K_2Fe[Fe(CN)_6]} + \underset{\mathrm{(yellowish)}}{\mathrm{In[Fe(CN)_6]}} \quad (3)$$

In a previous work [16], we demonstrated PIECD's blue-to-yellowish electrochromism with a coloration efficiency as high as ca. 103 cm^2/C at 690 nm, and the safe operating voltages for the fully bleached and fully colored states were determined to be 1.2 and 0 V (InHCF vs. PB), respectively. Furthermore, in order to fabricate an all-solid-state device, a K^+-doped solid polymer electrolyte (SPE), KCl-saturated poly-2-acrylamido-2-methylpropane sulfonic acid (AMPS), was employed. Although poly-AMPS (PAMPS) had been utilized as a proton-conducting SPE for two decades [25,26], we verified that the sulfonic matrix of PAMPS could also accommodate the conduction of K^+ after potassium doping [16]. Presumably, the conduction of K^+ in the PAMPS matrix is accomplished through the cationic exchange at AMPS's sulfonic ends or solvation of K^+ by the free water molecules residing in the SPE or both [27]. To date, we have successfully applied such a hybrid K^+/H^+ SPE not only to a PIECD but also to $PB-WO_3$ [28] and $InHCF-WO_3$ [27,29] electrochromic batteries.

Although it had been found that the PIECD using the K^+-doped PAMPS SPE achieves better cycling reversibility than the device using the pure PAMPS SPE [16], it has not been understood how much K^+ should be doped into the SPE to obtain the best performance. Thus, this work aims at finding out how SPE's KCl doping level affects the ECD performance. In this paper, we will first compare the at-rest stability of the PIECD with that of a precolored WO_3-PB ECD to illustrate the advantages of eliminating precoloration. Then the KCl doping level (defined by the molar ratio of KCl to AMPS in SPE, designated as (KCl)/(AMPS), in which (AMPS) was kept invariant) will serve as the dominant factor for discussions thereafter. The effect of doping level on the electrochemical behaviors, of both EC electrodes and the PIECD, will be discussed. Besides, the influence of (KCl)/(AMPS) on the transient transmittance, response time, transmittance window, coloration efficiency, and cycling reversibility of the PIECD will also be investigated. This work attempts to provide the basis for the optimal design on the K^+-SPE-based PIECD.

2. Experimental

All of the chemicals used in this work were reagent grade and were used as received without further purification. Deionized water (DIW) was used throughout this work. Unless especially noted, experiments were done at room temperature and in air. The experimental details are described below.

2.1. Substrate

Optically transparent F-doped SnO_2-coated (FTO) glass substrates ($R_{sh} = 20\ \Omega/\square$, Sinonar Corporation, Hsinchu, Taiwan) with dimensions of 5.0 × 2.5 × 0.2 cm were used as the conducting substrates for the electrodeposition of EC thin films. Before using, each FTO substrate was cleaned ultrasonically with 0.1 N HCl for 3 min and then rinsed with DIW. Afterward, a piece of Cu tape (3M Company, 2.5 × 0.5 cm) was applied to one side of the FTO-coated surface as the bus bar, and four pieces of insulating tapes were applied to result in an centralized, active area of 3.0 × 1.5 cm^2 for the thin-film electrodeposition.

2.2. Preparation of PB, InHCF, and WO_3 thin films

Prussian blue thin films were prepared by the galvanostatic electrodeposition. The deposition bath of PB contained 10 mM $FeCl_3$, 10 mM $K_3Fe(CN)_6$, 0.1 M KCl, and 1 M HCl. When preparing the PB thin film, a constant cathodic current density of 20 $\mu A/cm^2$ was applied to the FTO substrate for 700 s. Unlike the PB preparation, InHCF thin films were prepared via voltammetric electrodeposition [21]. The InHCF plating solution was prepared according to the stability-improved recipe [30] and was composed of 10 mM $InCl_3$, 10 mM $K_3Fe(CN)_6$, 1 M KCl, and 1 M HCl. While plating, a dynamic potential, scanned back and forth between 0.2 and 1.3 V (vs. Ag/AgCl/saturated KCl) at a rate of 200 mV/s, was exerted to the FTO substrate for 10 cycles (110 s). Both kinds of as-grown films were washed with DIW to remove the residual plating solutions and then were stored in air prior to use.

To compare the at-rest stability of a PIECD with that of a WO_3–PB ECD, WO_3 thin films were also prepared in this work. The WO_3 films were deposited potentiostatically onto FTO glass substrates. The deposition solution was composed of 36.7 vol.% peroxy–tungsten acid (PTA) solution, 30.3 vol.% DIW, and 33.0 vol.% isopropanol. The preparation of the PTA solution was described elsewhere [28]. For WO_3 deposition, a constant potential of -0.45 V (vs. Ag/AgCl/saturated KCl) was applied to the FTO substrate for 8 min. The as-grown films were washed with DIW and then were fired at 100 °C for 1 h before cell assembly.

2.3. KCl-doped poly-AMPS solid polymer electrolytes

The KCl-doped PAMPS SPEs were prepared by UV polymerization. The KCl-doped AMPS monomer solutions were prepared as follows. First, 9.4 g of AMPS monomer was dissolved into 10 ml of DIW, and 0.3 ml of tetra(ethylene glycol diacrylate) (TEGDA), the cross-linking agent, was dropped into the solution. Next, a selected amount of KCl was added to obtain the desired KCl doping level. Then the solution was stirred for 15 min at room temperature. Afterward, 0.01 g of benzoin methyl ether (BME), the initiator, was dissolved into the solution with another 15-min stirring. Finally, the KCl-doped AMPS monomer solution ready for UV curing was prepared. During polymerization, a KCl-doped AMPS monomer solution was filled in a rectangular casting mold with inner dimensions of 3.0 × 1.5 × 0.2 cm and was exposed to UV irradiation with an energy intensity of ca. 675 $\mu W/cm^2$ (Spectroline, SB-125) for 3 min.

In this work, four monomer solutions with different KCl concentrations (referred to as solutions (a), (b), (c), and (d)) were prepared purposely to obtain the SPEs with various K^+ doping levels. The KCl concentrations for these solutions were (a) 2.48 M (saturated), (b) 1.00 M, (c) 0.10 M, and (d) 0.01 M, respectively. Hence, these solutions led to four SPEs having different molar ratios of KCl to AMPS (denoted by (KCl)/(AMPS)), i.e., four KCl doping levels: (a) 0.546, (b) 0.220, (c) 0.022, and (d) 0.002. Basically, the molar ratio of (KCl)/(AMPS) can be regarded as a measure of the molar ratio of K^+ to H^+ in the SPE, since KCl and AMPS serve as the sources of K^+ and H^+, respectively. Throughout this paper, we purposely compare the PIECDs incorporating the above four SPEs. The electrical and physical properties of these SPEs were discussed in a separate paper [27].

2.4. Cell assembly of PIECDs and the WO_3–PB ECD

In order to study the influence of SPE's KCl doping level on the switching behavior of a PIECD, four devices were fabricated. These devices were composed of the same PB and InHCF electrodes but employed different KCl-doped SPEs as described above. For the convenience of explanation, these devices are referred to as cells (a), (b), (c), and (d), respectively. When assembling a PIECD, a blue PB film and a colorless InHCF film were positioned facing each other, and one of the SPEs was sandwiched in between. In addition, double-sided foam tapes (thickness = ca. 2 mm) were applied and surrounded the SPE to serve as spacers. Then the PIECD was clipped tightly without further sealing. The active area for each cell was 3.0 × 1.5 cm^2. It is noteworthy that neither PB nor InHCF was precolored prior to cell assembly. All of the as-assembled devices displayed blue color and showed an open-circuit voltage of ca. 0 V.

The WO_3–PB ECD, in combination with the KCl-saturated PAMPS SPE (SPE (a)), was also fabricated so as to compare it with the precoloring-free PIECD. The cell assembly of WO_3–PB ECD was similar to that of a PIECD, except with an additional precoloration step. Precoloration of WO_3 film was necessary to achieve the complementary WO_3–PB EC function [12,15], as prebleaching of PB is impossible in the presence of air. When implementing the precoloration, the colorless WO_3 thin film was polarized potentiostatically (− 0.5V vs. Ag/AgCl) to the blue H_xWO_3 state in the presence of the KCl-saturated PAMPS SPE.

2.5. Electrochemical and in situ optoelectrochemical measurements

Cyclic voltammetric (CV) analyses were carried out with a computer-programmable potentiostat/galvanostat (Autolab, model PGSTAT30). The three-electrode CV was used to characterize the PB and InHCF thin films in the presence of the KCl-doped PAMPS SPEs. The two-electrode CV was utilized to characterize the PIECDs assembled with different SPEs. In the three-electrode measurements, a silver wire and a platinum plate served as the pseudo-reference and auxiliary electrodes, respectively. In the two-electrode measurements, InHCF was set as the positive electrode and PB was the negative one.

Transient transmittances at 690 nm of the PIECDs and the WO_3–PB ECD, in response to potentiostatic operations, were monitored simultaneously. A UV–visible spectrophotometer (Shimadzu, model UV-1601 PC) was used to measure the transient transmittances at a device's central position. All of the transmittance values reported in this paper included the optical contribution from both the SPE and the two FTO substrates. For the potentiostatic operations, all of the PIECDs were bleached at 1.2 V and colored at 0 V; the WO_3–PB ECD was bleached at − 0.3 V and colored at 1.0 V (For the WO_3–PB ECD, PB was set as the positive electrode and WO_3 was the negative one). In situ optical measurements were carried out to evaluate the at-rest stability, switching characteristics, and dynamic stability of ECDs.

3. Results and discussions

3.1. At-rest stability of the precoloring-free PIECD

Our intent behind fabricating an ECD based on the pseudo-transparent InHCF thin film was to eliminate the precoloration of EC electrodes before cell assembly. Although a precoloring-free ECD may not provide as much coloration efficiency as a precolored device, better at-rest stability can be expected according to the decolorized-state assembly. Figs. 1 and 2 confirm this expectation by comparing the at-rest stability of a precoloring-free PIECD with that of a precolored WO_3–PB ECD. The at-rest stability is evaluated from the spontaneous fading of transmittance window (optical attenuation range) and charge capacity. From these figures, it can be seen that both the transmittance window and charge capacity of the WO_3–PB ECD fades at a much faster rate than those

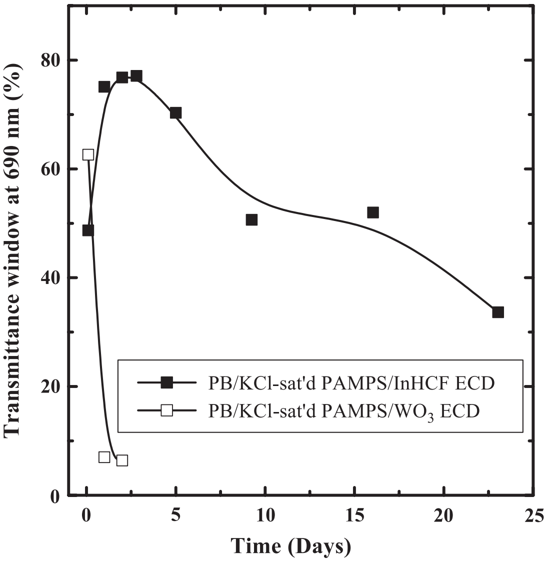

Fig. 1. Comparison between the spontaneous fading of PIECD's transmittance window and that of the WO_3–PB ECD. The experimental data were obtained under the following experimental conditions. PIECD: bleached at 1.2 V and colored at 0 V; WO_3–PB ECD: bleached at − 0.3 V and colored at 1 V; step time = 40 s.

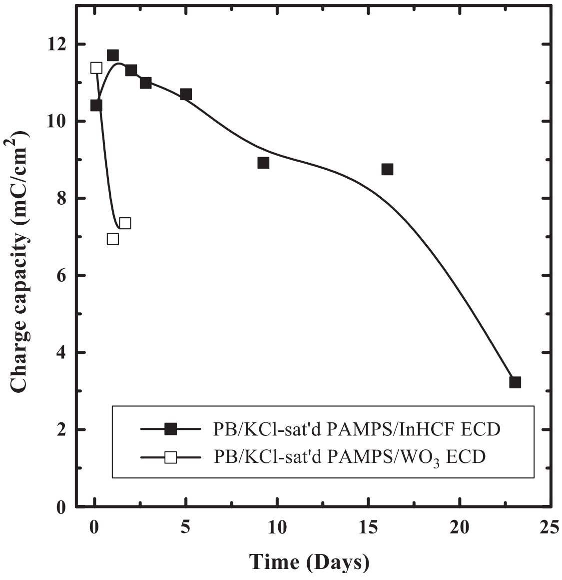

Fig. 2. Comparison between the spontaneous fading of PIECD's charge capacity and that of the PB–WO$_3$ ECD. The data were obtained under the same experimental conditions as described in Fig. 1.

of the PIECD. This implies that the precolored WO$_3$–PB ECD suffers from the at-rest instability much more seriously than the precoloring-free PIECD. In addition, the at-rest instability issue of the WO$_3$–PB ECD has to do with the partial oxidation of the precolored H$_x$WO$_3$ [15].

To achieve the EC switching complementary to the anodically coloring PB electrode, WO$_3$ was precolorized to the blue H$_x$WO$_3$ state in the presence of protons. However, H$_x$WO$_3$ in the assembled ECD was not stable in the presence of oxygen [15]. Thus, the precolored electrode self-discharged and returned to its relaxed state eventually. That is why the at-rest instability of the precolored WO$_3$–PB system is difficult to avoid, especially during the device fabrication process. As a result, the rapid fading on the EC performance is observed. On the contrary, neither PB nor InHCF had undergone precoloration before cell assembly, so the PIECD assembled from the non-precharged electrodes could exhibit better at-rest stability. Still, it is not clear as to why both the transmittance window and charge capacity of the PIECD reach maxima one day after cell assembly and then continues to decline (see Figs. 1 and 2).

3.2. Influences of SPE's KCl doping level on the PB and InHCF electrodes

Before investigating the influence of SPE's KCl doping level on the entire PIECD, the effects on individual EC electrodes were studied first, and the results are discussed here. Figs. 3 and 4 show how the SPEs with different KCl doping levels affect the CVs of the PB and InHCF electrodes, respectively. A similarity on both figures is that the peak potentials shift negatively when the KCl doping level decreases. Presumably, the shift reflects the K$^+$-dependent redox mechanisms, as expressed in Eqs. (1) and (2). When the concentration of K$^+$ in the SPE reduces, the redox potential of a metal hexacyanoferrate electrode shifts negatively according to the Nernst equation. Similar phenomena had been observed and reported for aqueous systems [17,31]. Apart from the similarity, the dissimilarity between the CV shapes is more obvious. By comparing these two figures, one finds that: the CV of PB becomes flat and small but remains relatively symmetrical as the KCl doping level decreases, whereas the CV of InHCF does not. InHCF can be discriminated from PB by the characteristics given blow: (i) the sharpest and highest redox waves occur in the case of (KCl)/(AMPS) = 0.220, not the saturation value at

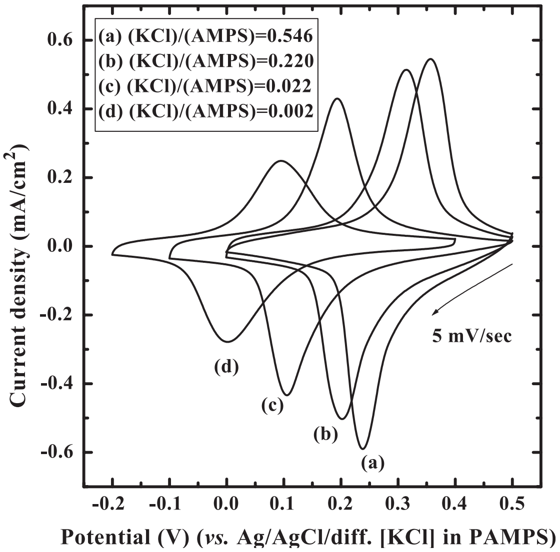

Fig. 3. Three-electrode CVs for PB under various SPE's KCl doping conditions. (KCl)/(AMPS) denotes the molar ratio of KCl to AMPS and serves as a measure of the KCl doping level.

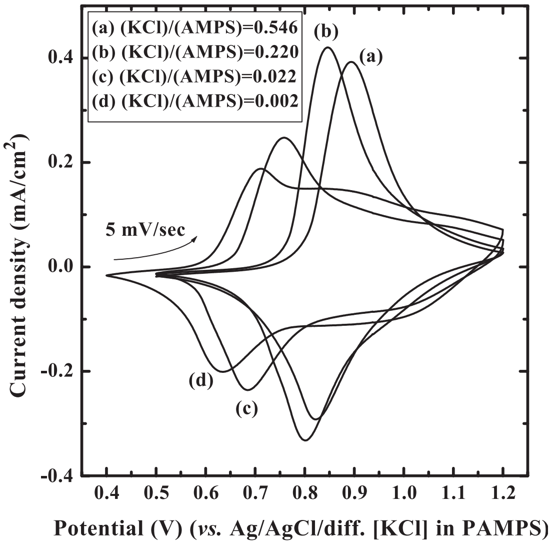

Fig. 4. Three-electrode CVs for InHCF under various SPE's KCl doping conditions.

0.546; (ii) low KCl doping levels (cases (c) and (d)) not only lead to flat CVs but asymmetry (case (d) even shows minor redox waves in the vicinity of 0.9 V).

The effect of the KCl doping level on PB's CV can be explained by PB's high selectivity for K^+. It is well known that PB strongly prefers K^+ for insertion kinetics and greatly resists the H^+ uptake [18,20]. Hence, it can be realized that the redox waves of PB become small and flat when K^+ concentration in the SPE becomes insufficient. Despite being an analog of PB, InHCF does not show as high a H^+ resistivity as PB, as judged by the data revealed in Fig. 4. To evidence this argument, Fig. 5 plots the charge capacities of PB and InHCF against the KCl doping level by integrating the CVs in Figs. 3 and 4. Fig. 5 unequivocally points out that the redox capacity of PB decreases as the KCl doping level decreases; however, the capacity of InHCF under low KCl doping conditions ((c) and (d)) can be maintained as high as (even higher than) that under high doping conditions ((a) and (b)). On the basis of this figure, we propose that InHCF prefers K^+ for its insertion kinetics but can also accept H^+ when K^+ concentration in the SPE is low. In fact, the relevant evidence can also be found in the literature [32]. Now, it is clear that the influences of the KCl doping level on PB and on InHCF are different. K^+ from KCl and H^+ from AMPS are competitive ions for InHCF rather than for PB. Thus, it can be expected that there must exist an optimal SPE's KCl doping level for achieving the best performance of the PIECD.

3.3. Influences of SPE's KCl doping level on PIECD's switching performance

This section discusses the effect of SPE's KCl doping level on PIECD's performance. Our studies started from the influence on ECD's electrochemical behaviors, characterized by the two-electrode CVs. Fig. 6 presents the CVs of the PIECDs assembled from the same electrodes but with different KCl-doped SPEs. Similar to the case of InHCF (see Fig. 4), the SPE in which (KCl)/(AMPS) = 0.220 leads to the sharpest and highest cell's voltammogram, which also implies the rapidest switching kinetics. This is consistent with the optical response results (in the form of transient transmittance) shown in Fig. 7. In this figure, cell (b) exhibits the widest transmittance window (63.2%↔7.4%) and fastest switching response (4.7 s for bleaching, 2.9 s for darkening). From Figs. 6 and 7, the coloration efficiency at 690 nm can be calculated. The calculated values are 111.0, 111.7, 85.4, and 85.6 cm^2/C for cells (a), (b), (c), and (d), respectively. Again,

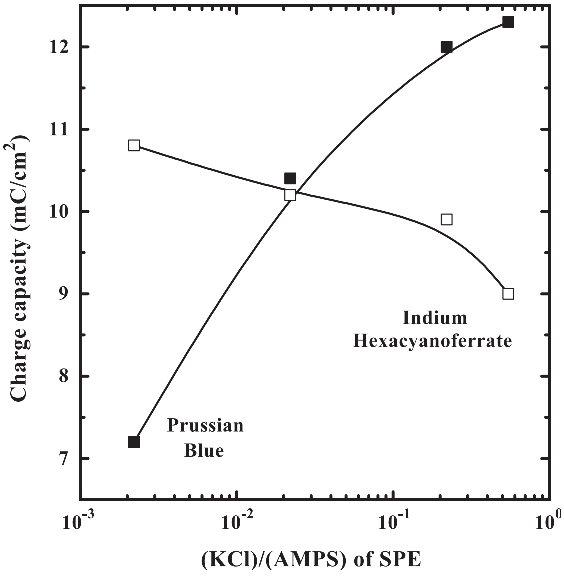

Fig. 5. Charge capacity values of PB and InHCF as a function of the KCl doping level. The capacity values were calculated by integrating the CVs in Figs. 3 and 4.

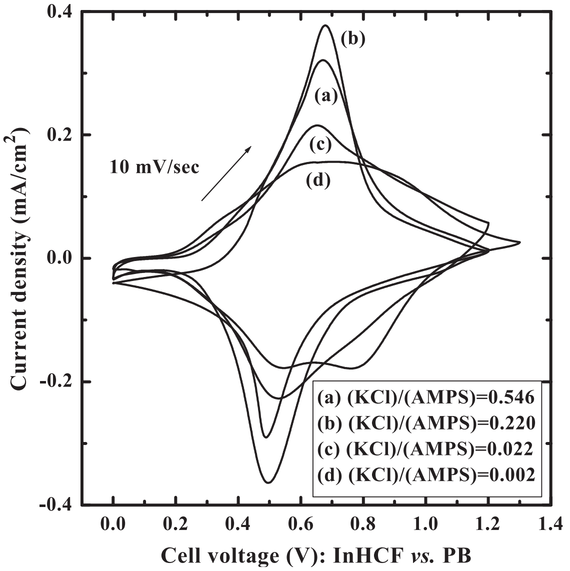

Fig. 6. Two-electrode CVs for the PIECDs assembled with different KCl-doped PAMPS SPEs.

it can be observed that cell (b) shows the highest coloration efficiency. Nonetheless, it may be more obvious to classify the coloration efficiency values into two groups: ca. 111 (cells (a) and (b)) and ca. 85 cm^2/C (cells (c) and (d)). By recalling that the influence of the doping level on a PIECD's CV is similar to that on InHCF, it can be deduced that the switching kinetics of the device are dominated by InHCF, rather than by PB. Furthermore, it had been mentioned that InHCF could steadily accept H^+ for insertion. Consequently, we presume that PB could suffer from the uptake of H^+ under low KCl doping conditions (cells (c) and (d)) for charge balancing against the InHCF electrode. And the lower coloration efficiency (85 cm^2/C) could have resulted from this non-favoured PB/ES switching mechanism. However, more evidence is needed to verify this presumption.

At first glance, the optimal SPE's KCl doping level for PIECD can be set at 0.220. Nonetheless, such a doping level does not yield the longest cycle life. By looking at Fig. 8, it can be observed that the cycle life of PIECD increases monotonically with the KCl doping level. The best cycling stability is obtained in the case of (KCl)/(AMPS) = 0.546, corresponding to the KCl-saturated PAMPS. This indicates that K^+ insertion is still the most favorable choice from the device's reversibility viewpoint, despite the fact that H^+ insertion could take place. As far as cycle life is concerned,

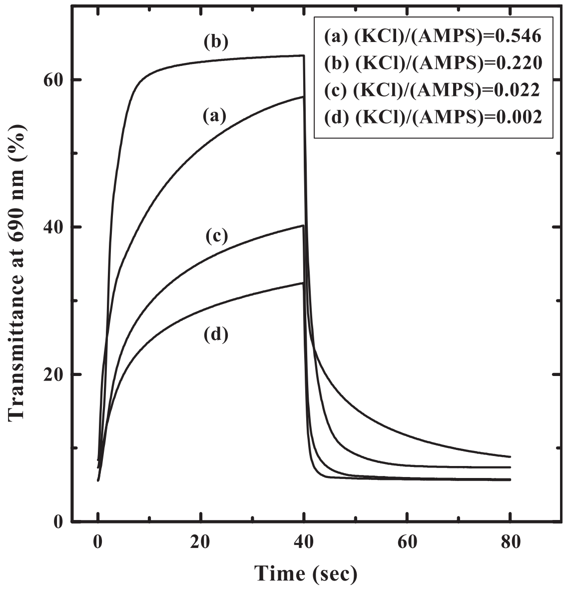

Fig. 7. Transient transmittances at 690 nm for the PIECDs using the KCl-doped PAMPS SPEs. All devices were bleached at 1.2 V and colored at 0 V potentiostatically.

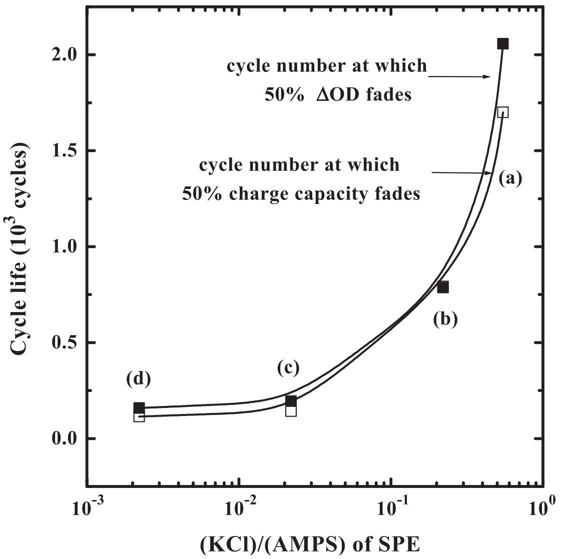

Fig. 8. Cycle life of the PIECD as a function of SPE's KCl doping level. Cycle life is defined as the cycle number at which 50% ΔOD (optical density change) or charge capacity fades. All devices were bleached at 1.2 V and colored at 0 V. The step time was 40 s for a measuring cycle and was 15 s for a switching cycle.

Table 1
The switching characteristics of the PIECDs assembled with the SPEs having different KCl doping levels

(KCl)/(AMPS) of SPE	$q_{\text{0V}\leftrightarrow\text{1.2 V}}$ (mC/cm^2)	τ_b (s)[a]	τ_d (s)[a]	$T_{690\ \text{nm}}$[b] (%)	$\eta_{690\ \text{nm}}$ (cm^2/C)	Cycle life[c] (× 10^3)
0.546	7.46	15.6	5.5	57.0↔8.5	111.0	2.06
0.220	8.35	4.7	2.9	63.2↔7.4	111.7	0.79
0.022	9.84	15.8	1.3	39.2↔5.7	85.4	0.19
0.002	8.76	15.2	0.9	31.5↔5.6	85.6	0.16

The data were calculated from Figs. 6–8.

[a] The time required for reaching 80% transmittance modulation. Superscripts b and d represent "bleaching" and "darkening", respectively.

[b] The optical contributions of FTO substrates and SPE are not excluded.

[c] Only the cycle numbers at which 50% ΔOD fades are shown.

efforts are still needed to improve the cycling stability of this system. Finally, to give an overall view of the SPE influence on the PIECD, Table 1 summarizes the quantitative results obtained from Figs. 6, 7 and 8.

4. Conclusions

According to the experimental results and the above discussions, the following four conclusions can be drawn from this work:

1. The precoloring-free PB–InHCF ECD, which is assembled from non-precharged EC electrodes, can ensure better at-rest stability in the presence of oxygen than a precharged system, such as the WO_3–PB ECD.
2. Although PB and InHCF both prefer K^+ for their insertion kinetics, InHCF may still allow H^+ uptake when SPE's KCl doping level is low. But PB tends to greatly resist the H^+ insertion.
3. The PIECD assembled with the SPE in which (KCl)/(AMPS) = 0.220 shows the fastest response, widest transmittance window, and highest coloration efficiency. Moreover, it is found that the switching kinetics of a PIECD is determined by InHCF rather than by PB.
4. PIECD using KCl-saturated PAMPS SPE shows the longest cycle life. This implies that a K^+-conducting SPE should be more favoured than a H^+-conducting SPE for the PIECD as far as cycle life is concerned.

Acknowledgements

The authors wish to thank Dr. S.C. Gau, Executive Vice President of Sinonar Corporation (Hsinchu, Taiwan) for providing the conductive F-doped SnO_2-coated glass substrates. This research was supported by the Program for Promoting Academic Excellence of Universities, sponsored by the Ministry of Education of the Republic of China, under grant no. Ex-91-E-FA09-5-4.

References

[1] P.M.S. Monk, R.J. Mortimer, D.R. Rosseinsky, Electrochromism: Fundamentals and Applications, VCH, Weinheim, Germany, 1995.
[2] R.D. Rauh, Electrochim. Acta 44 (1999) 3165.
[3] S.K. Deb, R.F. Shaw, U.S. Pat. No. 3,521,941 (1970).
[4] F.G.K. Baucke, D. Krause, B. Metz, V. Paquet, J. Zauner, U.S. Pat. No. 4,465,339 (1984).
[5] M. Mizuno, T. Niwa, U.S. Pat. No. 4,991,951 (1991).
[6] C.B. Greenberg, D.E. Singleton, US Pat. No. 4,768,865 (1988).
[7] S.K. Deb, Appl. Opt. Suppl. 3 (1969) 193.
[8] R.S. Crandall, P.J. Wojtowicz, B.W. Faughnan, Solid State Commun. 18 (1976) 1409.
[9] C.G. Granqvist, Sol. Energy Mater. Sol. Cells 60 (2000) 201.
[10] H. Tada, Y. Bito, K. Fujino, H. Kawahara, Sol. Energy Mater. 16 (1987) 509.
[11] M.A. Habib, S.P. Maheswari, M.K. Carpenter, J. Appl. Electrochem. 21 (1991) 203.
[12] K.-C. Ho, T.G. Rukavina, C.B. Greenberg, J. Electrochem. Soc. 141 (1994) 2061.
[13] P. Jelle, G. Hagen, R. Odegard, Electrochim. Acta 37 (1992) 1377.
[14] M.-C. Bernard, A. Hugot-Le Goff, W. Zeng, Electrochim. Acta. 44 (1998) 781.
[15] K.-C. Ho, Electrochim. Acta 44 (1999) 3227.
[16] L.-C. Chen, Y.-H. Huang, K.-C. Ho, J. Solid State Electrochem. 7 (2002) 6.
[17] D. Ellis, M. Eckhoff, V.D. Neff, J. Phys. Chem. 86 (1982) 4361.
[18] K. Itaya, T. Ataka, S. Toshima, J. Am. Chem. Soc. 104 (1982) 4767.
[19] R.J. Mortimer, D.R. Rosseinsky, J. Electroanal. Chem. 151 (1983) 133.
[20] K. Itaya, I. Uchida, V.D. Neff, Acc. Chem. Res. 19 (1986) 162.
[21] P.J. Kulesza, M. Faszynska, J. Electroanal. Chem. 252 (1988) 461.
[22] S. Dong, Z. Jin, Electrochim. Acta 34 (1989) 963.
[23] K.-C. Ho, J.-C. Chen, J. Electrochem. Soc. 145 (1998) 2334.
[24] R.E. Spindler, U.S. Pat. No. 5,209,980 (1993).
[25] J.-P. Randin, J. Electrochem. Soc. 129 (1982) 1215.
[26] R.D. Giglia, S.Y. Huang, U.S. Pat. No. 4,375,318 (1983).

[27] T.-S. Tung, L.-C. Chen, K.-C. Ho, Solid State Ionics, in press.

[28] L.-C. Chen, Y.-H. Huang, K.-S. Tseng, K.-C. Ho, J. New Mater. Electrochem. Syst. 5 (2002) 203.

[29] L.-C. Chen, K.-S. Tseng, Y.-H. Huang, K.-C. Ho, J. New Mater. Electrochem. Sys. 5 (2002) 213.

[30] L.-C. Chen, K.-S. Tseng, K.-C. Ho, J. Solid State Electrochem. 7 (2002) 1.

[31] M.A. Malik, G. Horanyi, P.J. Kulesza, G. Inzelt, V. Kertesz, R. Schmidt, E. Czirok, J. Electroanal. Chem. 452 (1998) 57.

[32] S.-M. Chen, J. Electroanal. Chem. 521 (2002) 29.